Modeling and Control of A Soft Circular Crawling Robot

Jiangnan Pang[1] Yibo Shao[1] Haozhen Chi[1] Yan Wu[2]

Abstract— **Soft robots have exhibited significant advantages compared to conventional rigid robots due to the high-energy density and strong environmental compliance. Among the soft materials explored for soft robots, dielectric elastomers (DEs) stand out with the muscle-like actuation behaviors. However, recently, modeling and control of a DE-based robot still remain further investigation because of the nonlinearity and viscoelasticity of DE actuators. This paper highlights the design, modeling and motion control of a soft circular robot which is capable of a 2D motion. To facilitate the design of a motion controller, a dynamic model of the robot is studied through a combination of theoretical analysis and experimental identification. For the motion control of the robot, a new PID plus feedforward control scheme is developed based on the model. Finally, the proposed model and control approach are verified through both simulations and experiments.**

I. INTRODUCTION

Recent developments in the field of robotics have led to a renewed interested in soft robots. Soft robots, made of compliant materials which are capable of continuous deformation, have a high degree of freedom and exhibit extremely high flexibility of movement. In contrast to conventional rigid robots, soft robots can achieve bio-inspired/bio-mimetic motions more easily, which have advantages in complex motion and environmental adaptability.

Soft actuators are obviously critical to soft robots. Several soft actuators for robotics have been proposed in previous work. Examples include shape memory alloy actuators (SMAs) [1], pneumatic/hydraulic actuators [2] and electroactive polymer actuators (EAPs) [3]. Dielectric elastomer actuators (DEAs), a kind of EAP actuators, show remarkable potential for robotic applications with large strain, fast response high energy density and similarity to biological muscle. These properties have contributed to developing bio-inspired/bio-mimetic soft robots.

A lot of efforts have been conducted in this field. The induced notable examples include several new humanoid robots inspired by DEAs [4], inchworm-like soft robots developed in [5] [6], and a circular-shaped soft robot manufactured in [7]. However, hitherto these soft robots are still a long way from practical applications. For example, the previous work about the circular-shaped soft robot mentioned in [7] only focuses on the materials and structures of the robot but ignores control system, resulting its merely open loop motion. In addition, the inchworm-like soft robot proposed in [5] is limited to its Ω-shaped structural constraints and can only perform a single-dimensional motion. From these studies, the main challenging of soft robots lies in the control issue due to the electromechanical coupling and viscoelasticity of the adopted soft materials.

This paper develops a DEA-based crawling soft robot capable of a omni-directional motion in 2D plane, and then the motion control issue is explored. The DEA, which consists of a thin elastomer membrane sandwiched between two compliant electrodes, is treated as the robot body and can achieve the deformation process with voltage-induced Maxwell stress [8]. While four electro-adhesion actuators (EAs) are adopted as the robot feet to provide adhesion force with the ground. To design a motion controller, a faithful plant model describing dynamics of the DEA is investigated. In the view of the similarity between DE materials and biological muscles, a knowledge-based data-driven modeling method is adopted, which could predict the dynamics of the robot wihtin the allowable error range and has a suitable form to meet the needs of controller design. Furthermore, a PID plus feedforward control scheme is proposed. The feedforward control system is used to expedite the response, and the feedback control method is employed to enhance the robustness of the system. Both simulations and experiments are adopted to prove that the precise control of the displacement can be realized quickly and accurately.

The remaining part of the paper proceeds as follows. In Section II are presented the mechanical design of the DEA-based circular soft robot and the locomotion mechanism. Section III describes how a dynamic model of the soft robot is built. In the next section, a feedforward plus feedback controller is employed to control the step length of this soft crawling robot. Finally, the paper concludes with the results of this investigation and a discussion of future research consideration in Section V.

II. THE SOFT ROBOT PROTOTYPE

A. Mechanical design of the robot

Figure 1 (a) shows the schematic of the designed robot. The robot is mainly composed of a circular-shaped DEA and four electro-adhesive actuators, wherein the circular-shaped DEA is used to control the extension and contraction of the soft robot, and the electro-adhesive actuators are employed for the adhesion between the substrate and the EAs during the movement. In addition, four passive omni-directional

This research is supported by the Agency for Science, Technology and Research (A*STAR) under its AME Programmatic Funding Scheme (Project #A18A2b0046).

Jiangnan Pang and Yibo Shao contributed equally to this work.

Haozhen Chi is the corresponding author.

[1]Jiangnan Pang (email: 13516857352@163.com), Haozhen Chi (email: 3150102315@zju.edu.cn) and Yibo Shao (email: 1427693687@qq.com) are with College of Control Science and Engineering, Zhejiang University, P.R.China 310027.

[2]Yan Wu (email: wuy@i2r.a-star.edu.sg) is with Institute for Information Research, A*STAR, Singapore.

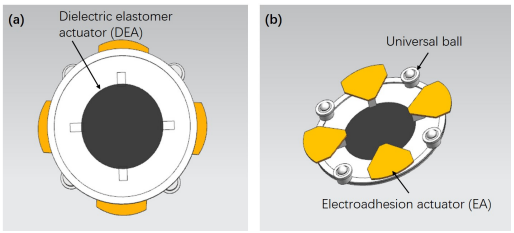

Fig. 1. Soft robot prototype

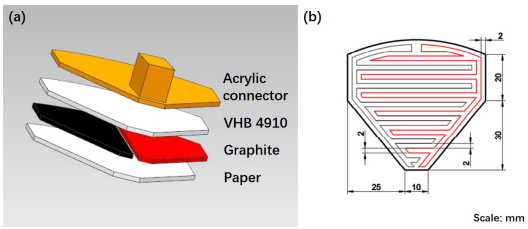

Fig. 3. The schematic of the robot foot

wheels are mounted on the robot to reduce frictional resistance during movement.

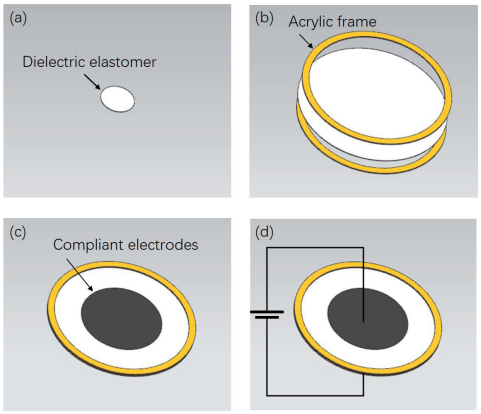

Fig. 2. The fabrication process of the DEA

Figure 2 presents the manufacturing procedure of the body portion of the robot. In the initial state, the membrane remains slack, which is a circle with a diameter of 50 mm and a thickness of 1 mm; then the membrane is stretched in an isotropic way and two annular acrylic frames are used to provide the desired mechanical constraint for the consummation of the pre-stretching. In this study, 4×4 biaxial pre-stretching is used, which makes the shape of the soft robot's body part a circle with a radius of 100 mm. The shape also ensures the uniformity of its orientation and simplifies the analysis process of subsequent research. Finally, both sides of the membrane are coated with carbon grease as electrodes to form an internal electric field and provide tensile stress. Figure 2 (d) illustrates the driving principle of DEAs. When the electrode area is subjected to a high voltage, the strain energy increases, which lead to a isotropic expansion of this area. When the voltage is removed, the electrode area will back to the original state. The minimum energy state of the DE-based system determines the actuation of the robot.

The foots of the robot is four electro-adhesion actuators which helps to adhere to the ground and achieve omni-directional motion. Figure 3 (a) gives the structure of the EA. The EA consists of three parts: electro-adhesive pad, VHB 4910 tape and acrylic connector to connect the foot with body. The EA is manufactured in the following manner: First, the pattern designed in Figure 3 (b) is printed on a A4 paper; Next, the graphite is painted with 2B pencil in the enclosed area as the electrodes; Finally, a piece of elastomer tape(VHB 4910) is used to connect the electro-adhesive pad and the acrylic connector as well as helps prevent short circuit of electrodes via external substance.

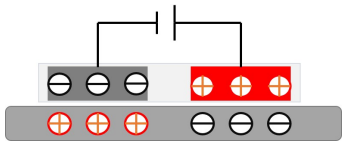

Fig. 4. Working principle of the EA

The mechanism of the electro-adhesion actuator is demonstrated in Figure 4. When a high voltage is applied, positive and negative charges accumulate on the respective electrodes. Simultaneously, inductive charges are generated on the surface of the ground. The different on the pad and the ground attract each other and thus produce electro-adhesion. With the voltage removed, the inductive charges disappear, as well as the electric field., leading to reversible adhesion [9].

B. Locomotion mechanism

Figure 5 (a) shows the number of four EA feet. Each of the EAs is powered by a voltage amplifier (EMCO Q101-5) which provides a voltage up to 10kV. And another amplifier(Dongwen) controlled by a micro-controller is adpoted to drive the DEA. An embedded micro-controller (Arduino UNO) is used to receive external sensor signals and calculate specific execution steps to control the specific actions of the robot through internal procedures.

Figure 5 (b) demonstrates the single-dimensional periodic motion of this soft robot, a specific cycle of the movement is as follows. At first, the EA_3 and DEA are driven, and the remaining EAs are not. Upon activation, EA_3 produces electro-adhesion force to fix itself on the substrate. At the same time, the robot body extends by the drive of DEA and pushes the EA_1 forward. Next, just power EA_1 while all the others in power loss, the DEA restores to its original state. Therefore, EA_3 is pushed toward the center. Repeating the above steps, the soft robot gradually moves forward cycle by cycle. Similarly, the soft robot can move backwards by reversing the actuation sequence of EA_1 and EA_3.

Benefiting from the isotropy brought about by the circular structure, the movement of the soft robot in two vertical directions is consistent. In other words, equipped with the other two EAs, the soft robot is able to move omni-directionally in the different actuation sequences. Figure 5 (c) shows the trajectory tracking motion in 2D plane. During the

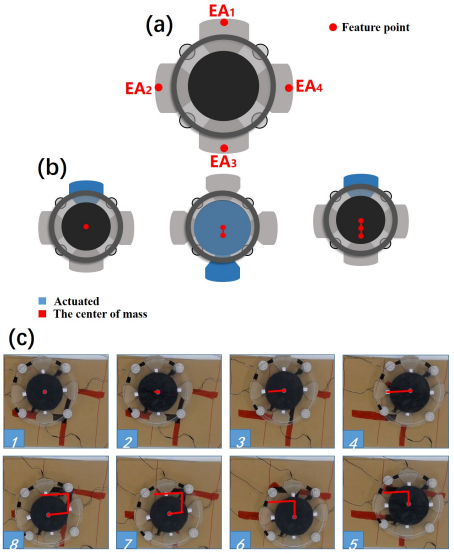

Fig. 5. The locomotion of the soft robot. (a) The feet number with the feature points; (b) the periodic movement; (c) the platform motion test experiment

experiment, an external camera has been used to obtain the red track information which would be sent to the controller, then the controller would adjust the motion mode of the soft robot with the feedback signals to realize a perfect tracking of the C-shaped trajectory. The final deviation of the experiment is small, which illustrates that the soft robot can achieve omni-directional motion by changing the sequence and interval of actuation.

III. Modeling of the Robot

It is essential to publish a faithful dynamic model before controller design. Previous modeling studies of DEA are generally based on the theory of DE or pure system identification. However, the models of these studies has limitations that do not adequately meet the requirements of the model-based control design. In this section, a knowledge-based data-driven modeling method is employed for the dynamic model of the DEA, as the method adopted in [10].

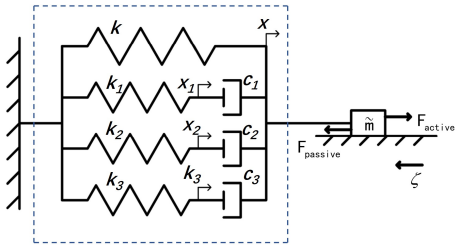

Fig. 6. The dynamic model of DEA based on spring-damper groups

Considering that this work only focuses on the changes of displacement and force between the two EA feet during the crawling of this soft robot, the points namely feature points shown in Figure 5(a) are situated as the junction between the EA feet and the DEA. Thus the distance change between the corresponding feature points are defined as the robot displacement, which makes the result more visible. In view of the similarity between DE materials and biological muscles, we use a spring-damper model mentioned in [11] to describe the single-dimensional physical properties of DEA. In Figure 6, a schematic of spring-damper groups is adopted to represent the dynamic characteristic. The form of the spring-damper groups is mimicked from the work of [11]. The model framework has also been adopted for the ω-shaped soft robots and proved to be able to well predict the dynamics of the DEA[12][13]. In the model framework, the spring with sitffness k is used to described the static stretch force. The spring deformation x_h, the spring stiffness k_h and the viscous friction coefficient c_h (h=1,2,3) are spring-damper parameters and describe the viscoelastic behavior. The uncertainties of the model are taken into account in terms of the equivalent mass $\tilde{m}$ of the system and the resistance ζ. Thus, the equations of dynamics are wrriten as

$$\tilde{m}\ddot{x} = -kx - \sum_{h=1}^{3} k_h x_h + F_{active} - \zeta sign(\dot{x}), \tag{1}$$

$$k_h x_h = c_h(\dot{x} - \dot{x_h}), h = 1, 2, 3. \tag{2}$$

The voltage induced force F_{active} can be thought of as the effect of the equivalent Maxwell stress and is also related to equivalent cross-sectional area of the body. Since Maxwell stress is a linear function of the electric field squared, F_{active} can be given by

$$F_{active} = g(x)V^2, \tag{3}$$

where the voltage V is applied in kV, $g(x)$ describes the effect of the displacement x. And during the experiment, we finally found that $g(x)$ is a linear function, so the formula above can be rewritten as

$$F_{active} = V^2(\alpha x + \beta), \tag{4}$$

where α and β are the coefficients of the first-order polynomial, the units are $N \cdot cm^{-}1 \cdot kV^{-2}$ and $N \cdot kV^{-2}$. The specific value will be obtained by experimental methods.

By converting the above differential equations into a state-space model, we can get

$$\begin{cases} \dot{X} = AX + Bu \\ y = CX \end{cases} \tag{5}$$

where

$$u = \frac{F_{active} + \tilde{f}}{\tilde{m}}, F_{active} \geq 0, \tag{6}$$

$$\tilde{f} = -\zeta sign(\dot{x}), \tag{7}$$

$$X = \begin{bmatrix} x_1 & x_2 & x_3 & x & \dot{x} \end{bmatrix}^T, \tag{8}$$

and

$$A = \begin{bmatrix} -k_1/c_1 & 0 & 0 & 0 & 1 \\ 0 & -k_2/c_2 & 0 & 0 & 1 \\ 0 & 0 & -k_3/c_3 & 0 & 1 \\ 0 & 0 & 0 & 0 & 1 \\ -k_1/\tilde{m} & -k_2/\tilde{m} & -k_3/\tilde{m} & -k/\tilde{m} & 0 \end{bmatrix}, \quad (9)$$

$$B = \begin{bmatrix} 0 & 0 & 0 & 0 & 1 \end{bmatrix}^T, \quad (10)$$

$$C = \begin{bmatrix} 0 & 0 & 0 & 1 & 0 \end{bmatrix}. \quad (11)$$

The spring-damper coefficient k_h and c_h are obtained through experimentally identification. Figure 7 demonstrates the experimental setup. One EA foot is fixed with a force sensor while the others are free and a camera is used to record the length change between these two EA feet.

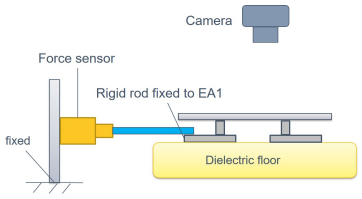

Fig. 7. The experiment setup for system identification

During the identification experiment, the DEA is firstly driven by an identification signal as the sinusoidal voltage sweep signal with the frequency of 0.2∼1 Hz, the amplitude of 0.36 kV and the offset of 3kV. Then, the parameters in equations are estimated through MATLAB System Identification Toolbox. The identification result is shown in Figure 8 (a). After the identification, several basic signals (sinusoidal and triangular signals) of different frequencies are employed to verify the identified model, and the results are displayed in Figure 8 (b) and Figure 8 (c).

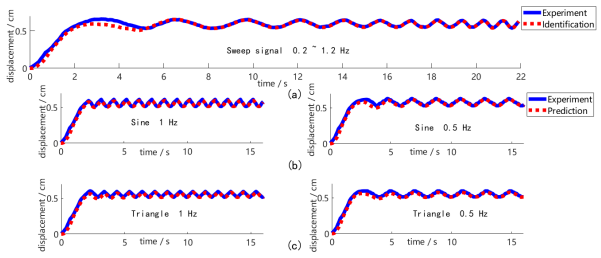

Fig. 8. The result of the model identification and validation. (a) The identification result applying a sweep voltage signal. (b) and (c) are validation results of sinusoidal and triangular signals, respectively.

As can be seen from the curves shown above, the simulated curves do not exactly match the actual curve, while there is always a slight lag during the initial phase of the response. There are two reasons for this deviation: (1) there is a deviation in the model identification process, especially with a linearization operation applied to the actual model; (2) the inherent viscoelastic with other properties of the DE material will cause the model uncertainties, which cannot be predicted and eliminated during the modeling process. Therefore, this deviation cannot be corrected by barely model parameter adjustment, and the existence of the deviation makes it impossible to directly obtain the desired output response through the input signal.

Among the parameters to be identified, the stiffness k mainly describes the elastic properties under static conditions, α and β mainly represent the electromechanical coupling relationship, $\tilde{m}$ reflects the mass of the robot platform itself, and ζ is mainly dependent on static properties such as friction coefficient when considering only low-speed motion. The spring stiffness k_i and the viscous friction coefficient c_i determine the robot's dynamic characteristics, reflecting the viscoelasticity and creep property.

TABLE I
THE IDENTIFICATION MODEL PARAMETERS

$\tilde{m}(kg)$		0.12	
$\zeta(N)$		$0.1\tilde{m}g$	
$k(N \cdot cm^{-1})$		3.456	
$\alpha(N \cdot cm^{-1} \cdot kV^{-2})$		3.6	
$\beta(N \cdot kV^{-2})$		-0.25	
$k_1(N \cdot cm^{-1})$	34.64	$c_1(N \cdot cm \cdot s^{-1})$	0.4
$k_2(N \cdot cm^{-1})$	15.2	$c_2(N \cdot cm \cdot s^{-1})$	5.067
$k_3(N \cdot cm^{-1})$	0.0396	$c_3(N \cdot cm \cdot s^{-1})$	12

Finally, the identified parameters are listed in Table I. In addition, the equivalent mass $\tilde{m}$ is 0.12 kg and the resistance ζ is estimated to be $0.1\tilde{m}g$, where g is the gravity coefficient. From the validation results, the identification model is well matched with the actual model, and can well predict the creep under different voltage signals.

According to the measured data, the fit of above-mentioned curves are all more than 85%, which has reached the expected level while the complete matching is impossible due to the model uncertainties. Hence, in order to optimize the input-output relationship and realize the precise control of the soft robot, it is necessary to add an appropriate controller to effectively compensate the deviation.

Obviously, the model developed in this paper is completely a simplified version compared to the actual model of DEA. However, it will be more suitable for the DEAs considering the expense of the modeling cost. And the complex models are always difficult to apply to actual control, while simplified models are apposite for control problems of complex geometric DEA that are difficult to analyze or describe. Therefore, in the consideration of the principle of universal significance and convenience, we finally adopt the above simplified model to design the control scheme.

IV. Control of the Robot

In this work, our target is to achieve the set displacement control of the step length, which would be implemented by the PID-based feedforward-feedback controller as mentioned in [14]. Regarding the specific implementation, the working mechanism of this controller is as follows. First, the feedforward controller dominates to minimize the response

time so that the system state will quickly approach the set point. When the error is within a small range, the PID feedback controller begins to play a leading role to ensure a high accuracy with robustness, and finally achieves precise control.

A. Feedforward controller

Since four passive omni-directional wheels are used to reduced the friction, the resistance force $\tilde{f}$ can be ignored in the feedforward design and be compensated by the feedback control. The dynamic model we developed in (5) can be written as follows

$$\begin{cases} \dot{X} = AX + B\tilde{u} \\ y = CX \end{cases} \tag{12}$$

with

$$\tilde{u} = V^2(\alpha x + \beta) \tag{13}$$

where $\tilde{u} = V^2(\alpha x + \beta)$ is considered as the equivalent input of the DEA and helps linearize the nonlinear soft robot system.

To design the feedforward controller, the linearized state-space model is changed into the transfer function:

$$G(s) = \frac{Y(s)}{\tilde{u}} = C(sI - A)^{-1} + B. \tag{14}$$

Therefore, based on the inverse model, a feedforward controller is developed:

$$G_{ff} = G^{-1}(s). \tag{15}$$

However, G_{ff} is not an implementable controller. Thus, a second order low-pass filter $Q_f(s)$ is added to make it an implementable system:

$$Q_f(s) = \frac{1}{s^2/\omega_n^2 + s/(q\omega_n) + 1}, \tag{16}$$

with a high cutoff frequency selected that is much greater than the reference frequency. Thus, the model-based feedforward controller is developed as:

$$U_{ff} = Q_f G^{-1} X_d, \tag{17}$$

where X_d is the desired displacement.

B. Feedback controller

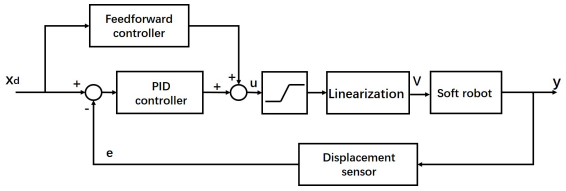

Fig. 9. The scheme of the PI controller with feedforward

To eliminate the lumped disturbance including the resistance force and enhance the robust of the system, the actual displacement information is used and a PID controller is designed:

$$u_{fb}(t) = K_p[e(t) + \frac{1}{T_i}\int_0^t e(\tau)d\tau + T_d\frac{de(t)}{dt}] \tag{18}$$

where $e(t) = y_d(t) - y(t)$ is the displacement error, K_p is proportional gain, T_i is the integral coefficient and T_d is the differential coefficient.

Thus, we developed a PID-based feedforward-feedback controller, as Figure 9 shows. Therefore, the feedforward-feedback control strategy could achieve a better consequence.

V. Simulations and Experiments

To verify the efficiency of the proposed feedforward-feedback controller, both simulations and experiments are conducted in this section.

A. Simulations

According to the feedforward-feedback control scheme described above, the precise control of the set displacement is simulated under the MATLAB Simulink Tool, while the dynamic model in Section III is adopted as the objected model. Considering the stretch limitation of the actual model and the current upper limitation of the voltage that can be supplied (breakdown voltage and boost module maximum output), we need to set the desired displacement as "physically reachable" for comparison with subsequent experimental data.

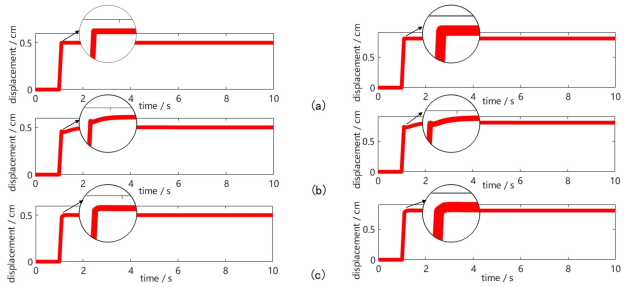

Fig. 10. The simulation results to control different step lengths through different controller. (a) Feedforward controller. (b) PID controller. (c) PID controller with feedforward.

As shown in Figure 10, we set the displacement to 0.5cm and 0.8cm respectively, and then compare the control effectiveness under the three control schemes of feedforward, feedback and feedforward-feedback control. It can be found that the response speed under the feedforward control scheme is really fast, but there is an obvious "hard turning", which cannot be realized in the actual object. Therefore, the feedforward scheme may be applied to the soft robot with large distortion, and the "hard turning" may cause problems such as oscillation and breakdown. Simultaneous, the feedback control scheme has a slower response, but with a smoother trajectory, which can be implemented. However, the feedforward-feedback control scheme reflected by Figure 10 (c) well combines the advantages of the feedforward and the feedback control schemes, presents a

superior performance. Its response speed is similar to the feedforward control scheme, but there is a smooth transition at the "hard turning point", which belongs to the "physically achievable" transition trajectory. Therefore, the feedforward-feedback control scheme is undoubtedly the best scheme among these three.

In summary, with the feedforward-feedback controller, the simulation results indicate that the control scheme proposed above performs well on the precise displacement of the soft robot.

B. Experiments

To verify the effectiveness and feasibility of the proposed feedforward-feedback controller, several experiments for different set displacement are conducted in a wooden desk with the size of 1 $\times$ 1.6 m. The experimental platform is the soft robot detailed in Section II.

For specific experimental steps: firstly, fix the rear foot (EA_3 for example) and make the others at a freely moving state; secondly provide control signals to control the input voltage according to the internal algorithm through the embedded micro-controller (Arduino UNO), while the soft robot will deform and shift which occurs the displacement. The displacement generated during the actual operation can be obtained by determining the moving distance of the front foot. For the detection of the displacement, because the experiment is relatively simple, the external camera can be perfectly captured with the basic object recognition program.

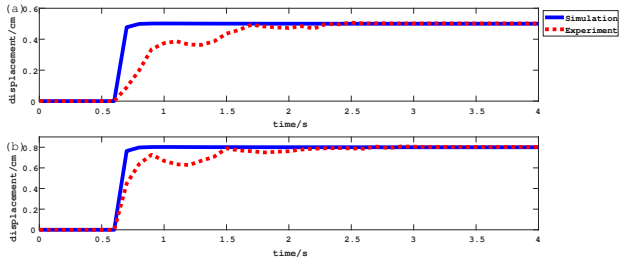

Fig. 11. The control results of simulation and experiment ($k_p = 800$, $k_i = 500$, $k_d = 70$).

Figure 11 shows the simulation results and experimental results for different setting displacement as 0.5 cm and 0.8 cm. Due to the simplified modeling method and the model uncertaintied caused by viscoelasticity and nonlinearity, the identification model cannot match the experimental data in the transient response phase. It should also be pointed out that in the process of adjusting the PID parameters, the overshoot ratio in the traditional sense is not used as the adjustment basis, but it is intentionally kept in an underdamped state to prevent the increasing voltage from reaching the "breakdown voltage", which leads to the collapse of the robot platform. So this curve is also based on safety considerations. However, in the steady state phase, the two can be matched perfectly. So the control effect is appropriate on the set point control problem.

VI. Conclusion

This paper demonstrates the design of a crawling soft robot with DEA as the main actuator. The soft robot equipped with a DEA and four EAs shows excellent 2D mobility. To design the controller for this soft robot, we employed a novel model method via both physical analysis and experimental identification. The properties of the circular DEA are described with a model usually used for biological muscle. Compared to the pure analytical model, this model is much simpler and more suitable for controller design at the expense of little precision. It takes viscoelasticity and friction into consideration and can predict the dynamic response of the DEA within the tolerance of error. Based on the faithful dynamic model, a PID plus feedforward control scheme is adopted to achieve the set displacement control of the soft robot.

References

[1] S. Seok, C. D. Onal, K. J. Cho, R. J. Wood, D. Rus, and S. Kim, "Meshworm: A peristaltic soft robot with antagonistic nickel titanium coil actuators," *IEEE/ASME Transactions on Mechatronics*, vol. 18, no. 5, pp. 1485–1497, 2013.

[2] D. Marcheseandrew, D. Onalcagdas, and RusDaniela, "Autonomous soft robotic fish capable of escape maneuvers using fluidic elastomer actuators," *Soft Robotics*, vol. 1, no. 1, p. 75, 2014.

[3] Q. Shen, S. Trabia, T. Stalbaum, V. Palmre, K. Kim, and I. K. Oh, "A multiple-shape memory polymer-metal composite actuator capable of programmable control, creating complex 3d motion of bending, twisting, and oscillation," *Scientific Reports*, vol. 6, p. 24462, 2016.

[4] J. W. Kwak, H. J. Chi, K. M. Jung, J. C. Koo, J. W. Jeon, Y. Lee, J. D. Nam, Y. Ryew, and H. R. Choi, "A face robot actuated with artificial muscle based on dielectric elastomer," *Journal of Mechanical Science and Technology*, vol. 19, no. 2, pp. 578–588, 2005.

[5] J. Cao, Q. Lei, J. Liu, Q. Ren, C. C. Foo, H. Wang, H. P. Lee, and Z. Jian, "Untethered soft robot capable of stable locomotion using soft electrostatic actuators," *Extreme Mechanics Letters*, vol. 21, pp. 9–16, 2018.

[6] L. Xu, H. Q. Chen, J. Zou, W. T. Dong, G. Y. Gu, L. M. Zhu, and X. Y. Zhu, "Bio-inspired annelid robot: a dielectric elastomer actuated soft robot," *Bioinspiration & Biomimetics*, vol. 12, no. 2, p. 025003, 2017.

[7] L. Qin, Y. Tang, U. Gupta, and J. Zhu, "A soft robot capable of 2d mobility and self-sensing for obstacle detection and avoidance," *Smart Materials and Structures*, vol. 27, no. 4, 2018.

[8] A. Ohalloran, F. Omalley, and P. Mchugh, "A review on dielectric elastomer actuators, technology, applications, and challenges," *Journal of Applied Physics*, vol. 104, no. 7, p. 071101, 2008.

[9] J. Shintake, S. Rosset, B. Schubert, D. Floreano, and H. Shea, "Versatile soft grippers with intrinsic electroadhesion based on multifunctional polymer actuators," *Advanced Materials*, vol. 28, no. 2, pp. 205–205, 2016.

[10] H. E. Xiao-Yang, L. I. Jian, L. Min, Y. X. Han, and J. X. Duan, "Modeling of distillation column based on hybrid neural network and prior knowledge," *Control Engineering of China*, 2009.

[11] G. Y. Gu, U. Gupta, J. Zhu, L. M. Zhu, and X. Zhu, "Modeling of viscoelastic electromechanical behavior in a soft dielectric elastomer actuator," *IEEE Transactions on Robotics*, vol. PP, no. 99, pp. 1–8, 2017.

[12] J. Cao, W. Liang, J. Zhu, and Q. Ren, "Control of a muscle-like soft actuator via a bioinspired approach," *Bioinspiration and Biomimetics*, vol. 13, no. 6, 2018.

[13] J. Cao, W. Liang, Q. Ren, U. Gupta, F. Chen, and J. Zhu, "Modelling and Control of a Novel Soft Crawling Robot Based on a Dielectric Elastomer Actuator," in *Proceedings - IEEE International Conference on Robotics and Automation*, 2018, pp. 4188–4193.

[14] X. Yuan, Y. Wang, and L. Wu, "Composite feedforward-feedback controller for generator excitation system," *Nonlinear Dynamics*, vol. 54, no. 4, pp. 355–364, 2008.